Journal of
Materials Chemistry C

ROYAL SOCIETY
OF CHEMISTRY

PAPER

View Article Online
View Journal

Cite this: DOI: 10.1039/d1tc05279a

Published on 30 March 2022. Downloaded by University of Bath on 4/11/2022 1:39:27 PM.

GaN LEDs with *in situ* synthesized transparent graphene heat-spreading electrodes fabricated by PECVD and penetration etching

Fangzhu Xiong,[a] Jie Sun,*[b] Matthew T. Cole,[c] Weiling Guo,*[a] Chunli Yan,[d] Yibo Dong,[a] Le Wang,[a] Zaifa Du,[a] Shiwei Feng,[a] Xuan Li,[a] Tailiang Guo[b] and Qun Yan[b]

Currently, applying graphene on GaN based electronic devices requires the troublesome, manual, lengthy, and irreproducible graphene transfer procedures, making it infeasible for real applications. Here, a semiconductor industry compatible technique for the *in situ* growth of patterned graphene directly onto GaN LED epiwafers for transparent heat-spreading electrode application is introduced. Pre-patterned sacrificial Co acts as both an etching mask for the GaN mesa and a catalyst for graphene growth. The Co helps in catalyzing the hydrocarbon decomposition and the subsequent graphitization, and is removed by wet etching afterwards. The use of plasma enhancement in the graphene chemical vapor deposition reduces the growth temperature to as low as 600 °C and improves the graphene quality, where highly crystalline graphene can be obtained in just 2 min of deposition. This method reduces the exposure of the GaN epilayers to high temperature to its limit, avoiding the well-known GaN decomposition and In segregation problems. Importantly, it can directly pattern the graphene without using additional lithographic steps and in doing so avoids any unintentional deleterious doping and damage of graphene from contact with the photoresist. The approach simplifies the fabrication and enables mass production by eliminating the bottlenecks of graphene transfer and patterning procedures. By comparing the GaN LEDs with and without graphene, we find that graphene greatly improves the device optical, electrical and thermal performances, due to the high optical transparency (91.74%) and high heat spreading capability of the graphene electrode. Unlike transferred graphene, this method is intrinsically scalable, reproducible, and compatible with the planar process, and is beneficial to the industrialization of GaN-graphene optoelectronic devices, where the integrated graphene serves as a superior sustainable and functional substitute to other transparent conducting materials such as ITO.

Received 2nd November 2021,
Accepted 28th March 2022

DOI: 10.1039/d1tc05279a

rsc.li/materials-c

1. Introduction

As a representative of third-generation semiconductors, gallium nitride (GaN) is a direct and wide bandgap (3.4 eV) semiconductor used extensively in a variety of optoelectronic devices that emit optically in the green, blue, and ultraviolet ranges.[1,2] GaN's typical applications include high-brightness light-emitting diodes (LEDs),[3] laser diodes,[4] solar cells[5] and high-electron-mobility transistors.[6] Its high breakdown voltage has made it well suited to high-power applications.[7] As p-doping of GaN is rather difficult, indium tin oxide (ITO) is often used as a transparent electrode material to improve both the current spreading and current injection.[8–10] There are fluorine-doped tin oxide (FTO) and other conducting oxides as well. Graphene is a two-dimensional material made up of sp^2 carbon atoms, which was first isolated by the Geim research team[11] in 2004 by mechanical exfoliation of bulk graphite. Single-layer graphene is only 0.335 nm thick, demonstrating broad and flat band optical transmission of up to 97.7%.[12–15] Single layer graphene has an electron mobility of up to 200 000 $cm^2\ V^{-1}\ s^{-1}$ at room temperature.[16] Compared to other transparent conductors mentioned above, graphene is much thinner, lighter, "greener", more resource abundant, chemically more stable, more mechanically flexible, and most importantly, with a much wider spectral range of transparency. These features

---

[a] *Key Laboratory of Optoelectronics Technology, College of Microelectronics, Beijing University of Technology, Beijing 100124, China. E-mail: guoweiling@bjut.edu.cn*
[b] *Fujian Science & Technology Innovation Laboratory for Optoelectronic Information of China, and College of Physics and Information Engineering of Fuzhou University, Fuzhou 350100, China. E-mail: jie.sun@fzu.edu.cn*
[c] *Department of Electronic and Electrical Engineering, University of Bath, Bath BA120BN, UK*
[d] *Department of Information and Automation, Library of Fuzhou University, Fuzhou 350108, China*

Published on 30 March 2022. Downloaded by University of Bath on 4/11/2022 1:39:27 PM.

make it very competitive in optoelectronics. Indeed, graphene is fundamentally more sustainable than ITO, as indium is increasingly scarce and expensive. The graphene process is relatively simple and cheap, and it is stable in an acid or alkali environment. Graphene has a broad band optical transmittance from ultraviolet all the way to infrared light. Furthermore, suspended single-layer graphene has a thermal conductivity of up to $5300\ \mathrm{W\ m^{-1}\ K^{-1}}$ at room temperature,[17] which gives it the additional function of being a thermal spreader, which is unmatchable by other transparent conductors. Therefore, for the application in future optoelectronic devices, we believe graphene provides much more possibilities than ITO.

Offering the opportunities for industrial deployment, copper foil based catalysis of graphene by chemical vapor deposition (CVD) is to date the most widely reported method for the production of highly-crystalline and large-area graphene thin films.[18–21] However, that highly catalytically active substrate used to support graphene growth is hardly appropriate for most electronic applications of graphene. That is because the metal foils are electrically conductive and one needs to transfer graphene for any practical use in electronics. A technically complex and inefficient process, the graphene transfer, typically requires very skilled users who can manually transfer samples. Automated transfer has recently been demonstrated[22,23] and, though it increases the throughput, nonetheless continues to produce transferred graphene that is wrinkled, holey, folded, and often significantly contaminated.[24–26] It can cause the deterioration of the optoelectronic characteristics of the as-prepared graphene. In addition, the inevitable contaminations trapped between graphene and p-GaN during the transfer process lead to a highly non-ideal interface, resulting in a large potential barrier therein. That adds even more difficulties in establishing an ohmic contact between the two materials which already have some work function mismatch even under an ideal interface condition ($\sim$7.5 eV for p-GaN[27] and $\sim$4.8 eV for CVD graphene[28]). As a result, the ability to directly grow graphene *in situ* on GaN epitaxial wafers is desperately desired, which will ultimately obviate the need for transfer, and in doing so establish a new and technologically valuable method for fabricating highly transparent electronic contacts that have negligible contamination. This approach lays important foundations towards the integration of graphene with standard III–V semiconductor technologies and has demonstrable value for a variety of other applications including silicon based integrated circuits. Although vital for integration, the *in situ* growth of graphene on GaN is very rarely reported in the literature due to what are considered incompatible growth conditions of GaN and graphene. Though graphene's unique properties technologically complement those of GaN, the typical high temperate ($\sim$1000 °C) growth conditions required for graphene growth have been seen to drive buckling and decomposition of the GaN substrate.[29] These trends are notable exacerbated under a hydrogen atmosphere[30,31] which are essential for amorphous carbon removal[32,33] and the production of highly graphitic films during graphene synthesis. Some progress has been made in reducing the temperature for graphene synthesis,[34–36] though often at the expense of a reduction in the graphene's crystallinity, and hence the optoelectronic properties. GaN is produced at high temperatures ($\sim$1050 °C) by metalorganic chemical vapor deposition (MOCVD), but it is only stable in the $Ga(CH_3)_3$ and excess NH_3 environment which prevents its decomposition. Establishing such an environment during the graphene CVD would nevertheless prevent graphene formation. In order to solve this contradiction issue, in this paper, we have used several strategies to deposit transfer-free highly crystalline graphene onto GaN without compromising the GaN epitaxial wafers. To achieve this, we have successfully reduced the graphene deposition temperature to as low as 600 °C whilst maintaining a D/G Raman intensity ratio of 0.1. The graphene deposition time has also been dramatically reduced, achieving full coverage of our substrate within as little as 2 minutes, based on a unique rapid-PECVD (plasma enhanced CVD) system specifically designed as the integrative growth tool for supporting temperature reduction during the sacrificial cobalt (Co) catalysis. Collectively, this new methodology has, for the first time, allowed for the in-line, foundry compatible, direct *in situ* deposition of high quality graphene on GaN epitaxial substrates and in doing so offers a much needed solution to an industry wide challenge.

Apart from copper, other metals such as platinum, nickel and cobalt are effective catalysts and have been shown to be able to support the growth of single- and multi-layered graphene by CVD.[37–42] These metals generally are more catalytically active than Cu, which we believe are well-suited for supporting the creation of new low-temperature graphene growth protocols. However, as discussed earlier, the industry desires a transfer-free graphene growth method, yet with reasonably high quality. That is, the ability to grow highly crystalline graphene by *in situ* CVD at technologically viable temperatures that support multi-technology integration remains elusive. In this work, we chose Co as the catalyst for graphene growth not only because it is an effective catalyst for the production of graphitic carbon,[43] but also because the lattice constant on the Co surface almost perfectly matches the in-plane lattice constant of graphene, although it is not very commonly used.[44] We use its high catalytic ability to obtain decent quality graphene even at reduced temperatures. No observable Co/p-GaN alloys are found under our conditions. In fact, even if there existed a small amount of Co-GaN alloy that could hardly be totally avoided, it would not be harmful to the operation of the devices, as it would support the creation of a good ohmic contact to the p-GaN.[45] Actually, Co is a known p-type dopant to GaN, which confirms GaN's tolerance, at least to some extent, of Co alloying.[44] That, in part, is a founding rationale for the use of Co as the graphene catalyst here. Hence, pre-patterned Co is used as a sacrificial layer to locally catalyze graphene growth. Importantly, the patterned Co is also used as a dry etching mask to produce the GaN mesas. This dual function of Co makes the outlined methodology unique and offers the ability to pattern both GaN mesa and graphene electrodes within a single patterning step. No additional lithographic processes are required to pattern graphene, dramatically simplifying the process and reducing the photoresist

This journal is © The Royal Society of Chemistry 2022

Published on 30 March 2022. Downloaded by University of Bath on 4/11/2022 1:39:27 PM.

induced contamination and doping of the graphene.[46] Co was finally removed by the so-called penetration etching, as reported herein, which allows us to get rid of the Co catalyst without damaging graphene. Based on this new process flow, we have patterned high-quality graphene grown *in situ* on commercial GaN LED epiwafers by PECVD. The process is repeatable, controllable, scalable and fully compatible with today's semiconductor planar process, without compromising the properties of the as-synthesized graphene associated with additional transfer and patterning processes. Scanning electron microscopy (SEM), Raman spectroscopy, electroluminescence (EL) spectroscopy, and thermal distribution measurements have shown that the devices have, herein, evidenced notable advantages of the transfer-free GaN-graphene LEDs over conventional manually-transferred samples. The results represent an important solution required for the integration of graphene with incumbent technologies, towards developing new hybrid GaN-graphene optoelectronics.

2. Experimental procedures

Commercial GaN LED epitaxial wafers grown on sapphire (Xiangneng Hualei Optoelectronic Corporation) were used as-received. Fig. 1 depicts the LED fabrication process flow. All substrates were first cleaned in boiling acetone (56.5 °C), and rinsed in isopropanol (IPA) and deionized water. A 200 nm Co (99.995% purity) thin film was then deposited and patterned on GaN (Fig. 1a) as a dry etching mask by lift-off lithography and sputtering, to define an array of 260 × 515 μm^2 mesas. Samples were then placed into an inductively coupled plasma (ICP) dry etcher, using $SiCl_4$ and Cl_2 at 8:64 sccm ratio to through etch p-GaN and multiple quantum well (MQW) to a depth of 1.2 μm to reach the heavily doped n-GaN, as shown in Fig. 1b. After forming the mesa array, graphene was grown on the patterned Co dry etching mask by cold-walled PECVD (Aixtron, Black Magic) at 600 °C at 6 mbar under a $CH_4/H_2/Ar$ (5/20/960 sccm) atmosphere. Note that graphene does not grow in Co-free areas, rendering automatic patterning of graphene, which is a neat and handy process for graphene patterning. Fig. 2a shows a schematic of the graphene growth system. Fig. 2b shows an optical micrograph of plasma during growth on a 2-inch GaN wafer.

In order to investigate the effect of the growth time and plasma power on graphene quality, 4 samples were grown for 2 min in 0, 10, 40, and 100 W AC (15 kHz) plasma, and 4 additional samples were grown for 20 s, and 1, 2, 5 min in 40 W AC (15 kHz) plasma, respectively. Note that we tried AC plasma at different frequencies, and also DC plasma with different waveforms, but under our conditions these changes had little effect on the final graphene quality. Raman spectra were acquired using a spectrometer (Renishaw Invia Raman Microscope operated at an excitation of a 532 nm laser), with the samples measured in triplicate at center points on each sample. Fig. 2c and d show the Raman spectra for the 8 samples.

Having obtained patterned graphene on Co, the Co catalyst needs to be removed so as to make the LED p-electrode transparent. Prior to its removal, a PMMA (poly(methylmethacrylate)) polymer layer was coated onto the sample and baked at 150 °C for 15 min. In our previous work,[47] we have developed a penetration etching method, which effectively removes Co without removing graphene. The PMMA thickness is submicron which is thin enough to allow water, etchants and products to pass through. That is how the metal is thoroughly etched. As the metal is patterned, the PMMA contacts the substrate between the patterns. These parts of the PMMA serve as anchors to firmly hold the PMMA film during wet etching. That is, the PMMA film is attached to both the graphene and the GaN substrate. Thus, following the complete Co dissolution, the PMMA mechanically binds graphene to the wafer ensuring that it naturally "lands" on the surface of p-GaN rather than floating away in the etching solution (Fig. 1f). PMMA was then removed in acetone, and directly patterned graphene on p-GaN was attained. The etching solution $CuSO_4 : HCl : H_2O$ = 10 g : 50 mL : 50 mL was used for the Co etching experiment. Ti/Au (15 nm/300 nm) p and n metal electrodes were then fabricated at once by lift-off lithography and sputtering, as shown in Fig. 1g. In order to make better

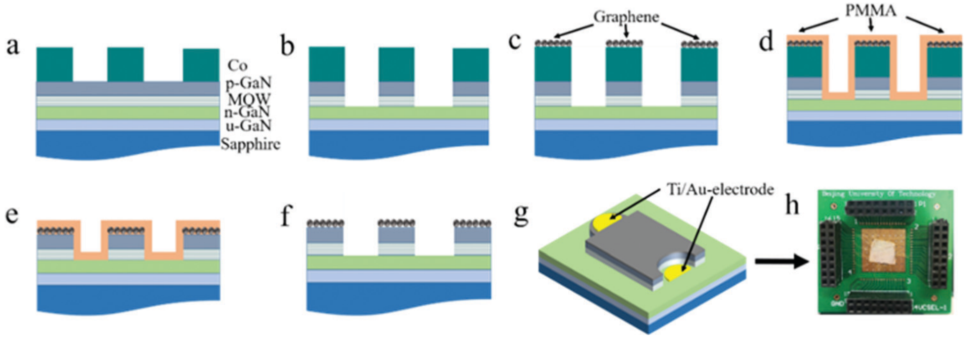

Fig. 1 GaN LEDs' transfer-free graphene integration process flow. (a) Patterned 200 nm Co thin film by lift-off lithography and sputtering. (b) Dry etched GaN wafer to reach the heavily doped n-GaN layer to form mesas. (c) Patterned graphene grown *in situ* on the Co catalyst. (d–f) Schematic illustration of the Co penetration etching removal process. The etchant peacefully penetrates the thin PMMA layer and removes Co, leaving behind the graphene which "lands" onto the GaN below. (g) Fabrication of Ti/Au (15 nm/300 nm) p and n metal electrodes by lift-off lithography and sputtering. (h) Wire bonding and packaging diagram of the LEDs. MQW represents multiple quantum well.

Published on 30 March 2022. Downloaded by University of Bath on 4/11/2022 1:39:27 PM.

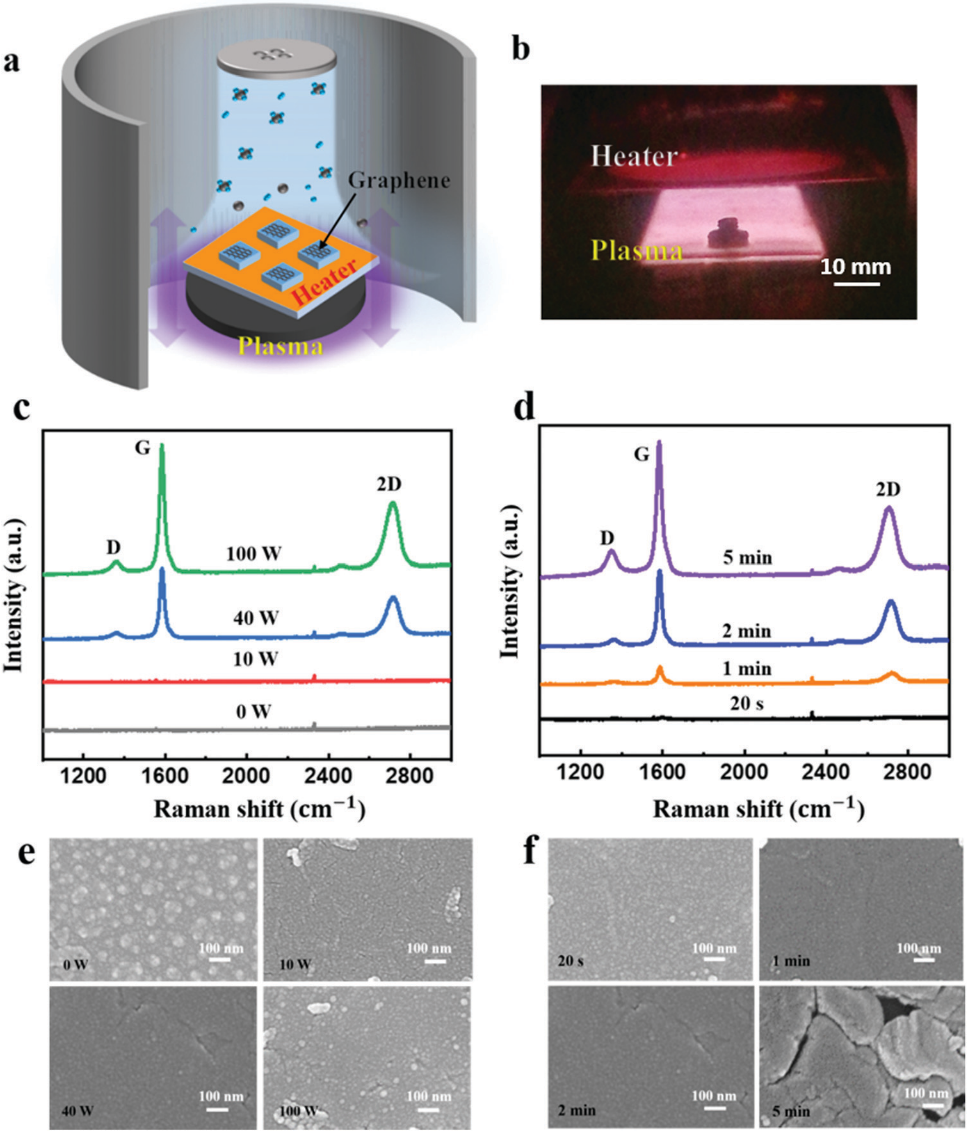

Fig. 2 (a) The graphene PECVD growth schematic. The gas ratio is methane : hydrogen : argon = 5 : 20 : 960. The growth temperature and chamber pressure are fixed at 600 °C and 6 mbar, respectively. (b) Photograph taken during the actual PECVD of graphene on GaN LED wafers, showing the glow map. (c) Typical Raman spectra of graphene subject to different AC (15 kHz) plasma powers for a deposition time of 2 minute. (d) Raman spectroscopy comparison of graphene grown for different time periods with 40 W plasma. (e) SEM images corresponding to the same samples measured in Fig. c. (f) SEM images corresponding to the samples in Fig. d.

contact among the metal electrodes, graphene, and p- or n-GaN, we annealed the final samples at 450 °C for 5 min under vacuum. The annealed LEDs were then bonded to a header package (gold-plated fiberglass) and encapsulated, as shown in Fig. 1h.

3. Results and discussion

As shown from Fig. 2c, a higher plasma power not only tends to allow graphene synthesis, but also plays an important role in enhancing the final quality of the synthesized graphene. Characteristic graphene spectral peaks does not appear until the plasma power reaches 40 W, corresponding to the positions of G and 2D peaks at 1585 cm^{-1} and 2719 cm^{-1}, respectively. The G and 2D peaks of graphene grown at 100 W plasma are located at 1584 cm^{-1} and 2715 cm^{-1}, respectively, which are almost identical to the former case. The intensities of these peaks, however, are known to reflect graphene quality as well as the number of layers.[48–50] The I(G)/I(2D) ratios are 1.67 and 1.80 for 40 W and 100 W plasma, respectively, which are rather similar values. The I(D)/I(G) ratios in both cases are approximately equal to 0.10. The I(D)/I(G) ratio is a known signature of the defect level.[51] The lower the ratio, the higher the crystalline quality. An I(D)/I(G) ratio of 0.10 is comparable to standard Cu-catalyzed graphene grown at 1000 °C.[52,53] Thus, our results indicate that under our conditions, in order to produce high quality graphene thin films at 600 °C, the plasma power needs to be reasonably large. If the power is too large, however, instead of increasing the

This journal is © The Royal Society of Chemistry 2022

Published on 30 March 2022. Downloaded by University of Bath on 4/11/2022 1:39:27 PM.

crystalline quality, it mainly increases the thickness. For example, the results at 40 W and 100 W plasma show similar D/G ratios indicating a similar quality, but at 100 W the G/2D is larger, suggesting a thicker film. On the other hand, the Raman analysis are only indicative of the quality and thickness and should not be taken as absolute conclusions. Fig. 2e shows the SEM images in accordance with Fig. 2c, which again confirms the importance of plasma for graphene growth. Although the samples grown at 0 W and 10 W plasma have not exhibited any detectable graphene Raman peaks, it can still be observed in the SEM images that the 10 W plasma-assisted sample grows faster than the plasma-free sample for forming a uniform film.

Fig. 2d shows the graphene Raman spectra for different growth times with 40 W plasma. No spectra can be acquired until the growth time reaches 1 min, upon which distinct G (1586 cm^{-1}) and 2D (2717 cm^{-1}) peaks appear, suggesting the formation of a graphitic thin film. For the growth time of 2 min, the G peak and 2D peaks can be clearly observed at 1583 cm^{-1} and 2720 cm^{-1}, while for 5 min growth, they appear at 1583 cm^{-1} and 2707 cm^{-1}. A comparison of the intensity ratio $I(\text{G})/I(\text{2D})$, 1.94 (5 min) $>$ 1.67 (2 min) $>$ 1.46 (1 min), indicates that the graphene thickness might increase over growth time, which is straightforward to understand. For a longer deposition time, the D peak intensity tends to increase, suggesting an increase in the number of defects. As shown in Fig. 2f, the SEM images corresponding to the samples measured in Fig. 2d, also demonstrate that the graphene film grown for 5 min appears to be thicker and with more cracks than the 2 min case. The gas composition, temperature, and pressure of the graphene growth have been systematically studied experimentally, and the optimal graphene growth conditions are found to be 600 °C, 6 mbar, with 100 W AC (15 kHz) plasma for 2 min, in a gas mixture of 5 sccm CH_4, 20 sccm H_2 and 960 sccm Ar. Under these conditions, a balance between the best possible graphene quality and maintaining the intactness of the GaN epitaxial layers and device structure has been reached.

Fig. 3a and b shows an optical microscopy image and a SEM image of the sample synthesized under the identified optimal conditions, respectively. The GaN epiwafer is seen to be intact @@with a rather smooth and clean surface after the graphene deposition. The graphene is seen to be continuous and covers the underlying p-GaN. In Fig. 3a, the lower left corner of the graphene is intentionally delaminated in order to make the p-GaN beneath visible. Fig. 3c represents the light transmission

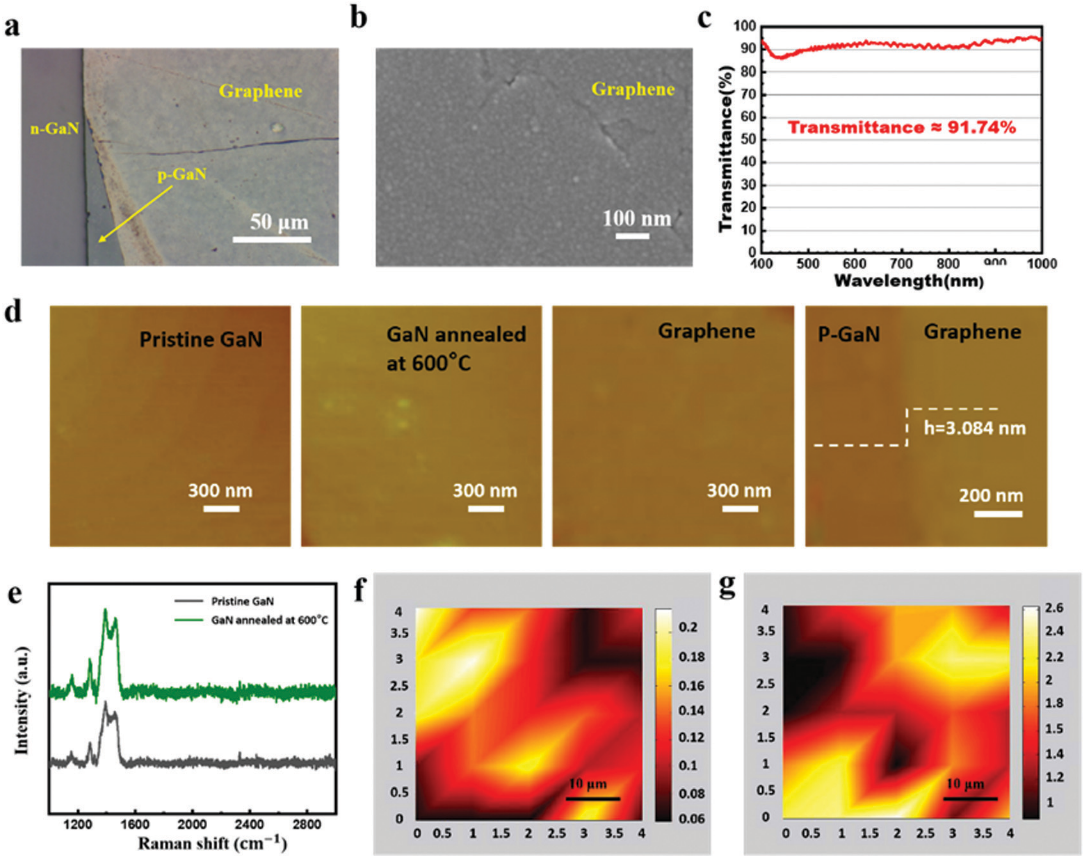

Fig. 3 (a) Optical image of the as-grown graphene on p-GaN. (b) SEM image of the graphene grown on p-GaN. (c) Optical transparency of the graphene transparent electrode situated on top of the GaN LEDs (the GaN substrate transmittance already subtracted) in 400–1000 nm. The average transmittance in this range is 91.74%. (d) AFM images of pristine GaN, annealed GaN, and graphene grown on GaN (the last two micrographs). (e) Raman comparison of the situation before and after the GaN annealing. (f and g) Raman mapping of the D/G and G/2D ratios of the graphene over a 40 µm × 40 µm area (5 × 5 points), respectively.

Published on 30 March 2022. Downloaded by University of Bath on 4/11/2022 1:39:27 PM.

of the sample, with an average transparency of 91.74% measured in the range of 400–1000 nm. In that measurement, the graphene-free sample was recorded first, and subtracted from the data of the GaN-graphene sample. Hence, what is illustrated in Fig. 3c is the value of bare graphene transparent conducting layer. Fig. 3d shows the atomic force microscopy (AFM) images corresponding to pristine GaN, GaN annealed at 600 °C, and the graphene grown on GaN as in Fig. 3b, respectively. Clearly, the GaN has not been damaged after the 600 °C growth, as judged from the AFM images. They correspond to an average surface roughness of 0.413 nm (GaN), 0.734 nm (GaN annealed), 0.422 nm (graphene grown on GaN), respectively. The nominal thickness of the as-deposited graphene film is about 3.084 nm measured by AFM. Fig. 3e shows the Raman curves before and after the annealing of GaN. It can be seen that although the growth temperature has been reduced to 600 °C, the roughness of the GaN surface still somewhat increases after the annealing, despite that they are not differing significantly in Raman characterization. Importantly, however, the graphene grown on GaN exhibits a lower roughness, which means that the graphene growth process help to maintain the surface quality of GaN to some extent. It can be understood as follows. The increase of the surface roughness is mainly because at high temperature the GaN tends to decompose and loose N element. However, when there are cobalt and graphene on it, they help to seal the GaN and reduce the nitrogen lost. Fig. 3f and g shows the Raman mapping result recorded from 1600 μm^2 area of the graphene surface, with D/G, G/2D ratios of 0.06–0.2 and 0.88–2.6, respectively, showing the reasonably high crystallinity and uniformity of the graphene films.

For graphene CVD, higher deposition temperatures generally give rise to higher crystallinity, increased morphology uniformity, and increased grain size.[54,55] Nevertheless, it is known that GaN based epitaxial layers are vulnerable to high temperature due to the GaN decomposition and the indium segregation in InGaN. Throughout our experiments, we have not noticed any deterioration of the GaN epiwafers, indicating that we have obtained a good balance between the quality graphene growth and the GaN intactness. To achieve this, first the graphene growth temperature is drastically reduced to 600 °C, which is built on our earlier work on the growth of graphene-like thin films on GaN.[56] During that earlier work, high growth temperatures of up to 950 °C were used, which was optically noted to damage the GaN. To obviate that issue in part, an NH_3 protection atmosphere was employed to prevent the GaN from losing N, deriving an NH_3-rich graphene growth environment. That method, however, compromised the quality of the synthesized carbonaceous material, resulting in a nano-graphitic matrix. That stimulated the exploration of alternative methods to realize the *in situ* growth of graphene on GaN. In the present work we opt to engineer the growth temperature within the indicative limit of 600 °C. Another important aspect of the outlined successful growth protocol is the short deposition time of just 2 minutes. Our graphene growth rate is probably one of the fastest reported to date, much faster than conventional Cu mediated graphene CVD. The graphene growth is extremely fast, where the entire growth experiment, even including pumping down, heating, cooling and venting, takes less than 25 min. Compared with the commonly used hot walled CVD systems which heat the entire quartz tube, our cold walled vertical CVD only heats the local heater, and the walls of the chamber are kept "cold". Thus, it can achieve rapid heating and cooling and improve the efficiency of growth, synthesizing high-quality graphene films in a short period of time. The time efficiency is certainly beneficial for mass production. Third, we use plasma enhancement to provide extra energy to the precursor molecules so that they can efficiently crack even at reduced temperatures, which help to boost the graphene quality at lower temperatures.

For comparison study, graphene-free samples, namely pristine and ITO coated (200 nm) GaN LED devices are also fabricated with an otherwise similar process to the GaN-graphene LEDs. The current–voltage (*I*–*V*) curve comparison is shown in Fig. 4. The turn-on voltages of the GaN-graphene LED, GaN-ITO LED and the pristine GaN LED are about 3.8 V, 4.8 V and 8.2 V, respectively, while the working voltages at 20 mA are about 4.1 V, 5 V and 7.6 V, respectively. The use of graphene tends to reduce the devices' characteristic voltages. In Fig. 4, the GaN-graphene LED already reaches 100 mA at 6.1 V. However, the same current level can only be reached in the

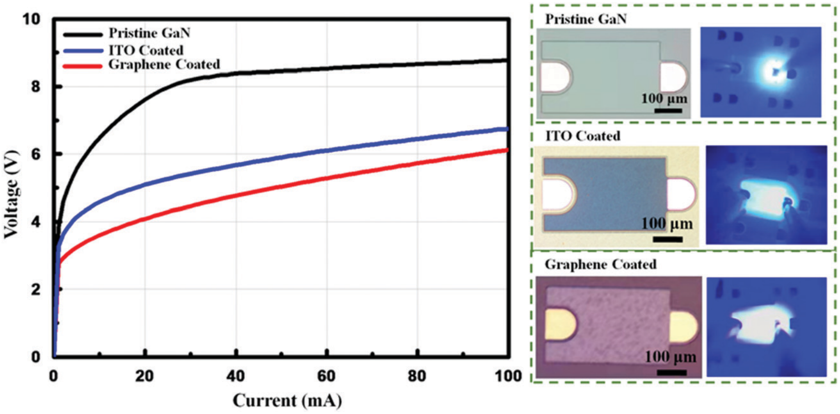

Fig. 4 A current–voltage curve comparison of different types of GaN LED devices. The pictures on the right show the corresponding optical images of their electroluminescence at 20 mA injection current.

Published on 30 March 2022. Downloaded by University of Bath on 4/11/2022 1:39:27 PM.

pristine and ITO coated LEDs when the voltage is as large as 8.8 V and 6.8 V, respectively. In Fig. 4, the pictures on the right are the corresponding optical images of the light emission at 20 mA, suggesting that the GaN-graphene LED illuminates with great uniformity. The light emitting area covers the entire p-GaN mesa for the GaN-ITO LED as well, but with a lower lighting intensity, whereas the pristine GaN LED has just one single light emission point located close to the p-electrode, a common phenomenon in higher-driving-voltage devices. The as-prepared graphene serves to enhance the functionality of the GaN LED by operating as an effective transparent conductive layer that shows an excellent current spreading effect, *i.e.* greatly improving the lateral surface conductivity of the GaN LEDs. We note that the thickness of the ITO layer here is the typical or even somewhat larger value compared to that of commercial GaN LEDs. Thus, at least under our experimental condition, the as-prepared graphene sample outperforms the standard ITO device.

Further quantitative data about the optoelectronic properties of graphene-on-GaN LEDs are explored *via* electroluminescence (EL) spectroscopy (Integrating sphere, EVERFINE) on the samples shown in Fig. 4. Fig. 5a and b shows the EL spectra from the different type of LEDs with injection currents of 20 mA and 100 mA, respectively, measured in the 380–780 nm range. Based on Fig. 5c and d, it can be seen that the GaN-graphene LED is superior to the pristine GaN LEDs in both the luminous flux and radiation flux. More specifically, the luminous flux values of the GaN-graphene LED are nearly twice as high as the pristine GaN LED both at 20 mA and 100 mA, which indicates an outstanding electrical to optical energy conversion efficiency in the GaN-graphene LED. These values are also significantly higher than those of the GaN-ITO LED. From the parameters shown in the table of Fig. 5e, in all the samples there is a notable blue shift of the order of 1 nm (GaN-ITO LED and the pristine GaN LED) and 1.6 nm (GaN-graphene LED) in the peak emission wavelength when the current is changed from

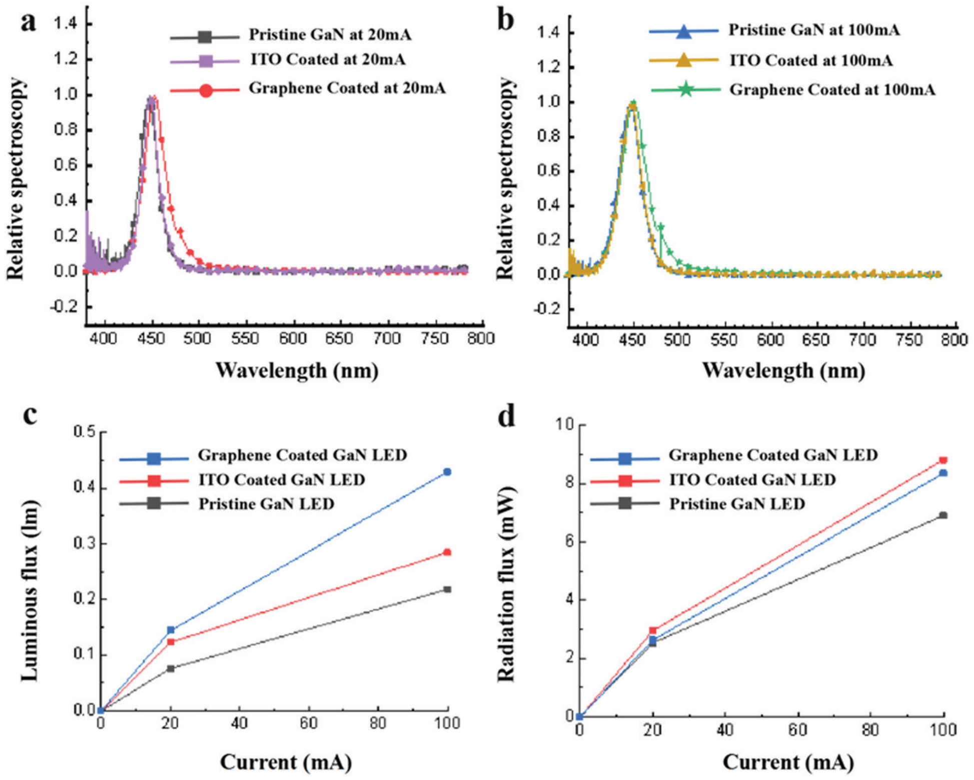

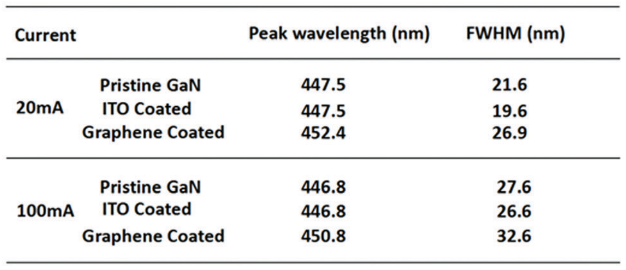

Current		Peak wavelength (nm)	FWHM (nm)
20mA	Pristine GaN	447.5	21.6
	ITO Coated	447.5	19.6
	Graphene Coated	452.4	26.9
100mA	Pristine GaN	446.8	27.6
	ITO Coated	446.8	26.6
	Graphene Coated	450.8	32.6

Fig. 5 Electroluminescence data of the three types of GaN LEDs measured at 20 mA and 100 mA injection current in the 380–780 nm range. (a and b) Relative intensity, (c) luminous flux and (d) radiation flux of the devices are plotted. (e) Is the corresponding spectral parameters.

View Article Online

Published on 30 March 2022. Downloaded by University of Bath on 4/11/2022 1:39:27 PM.

20 mA to 100 mA. It is known that the high built-in electric field (of the order of several MV cm^{-1}) along the (0001) direction of the InGaN/GaN quantum well[57] can induce the quantum confined Stark effect (QCSE) and lead to a red shift in the wavelength. When the injected current becomes large, however, due to the relatively long lifetime of the carriers (in the order of ns), they will accumulate in the quantum well, leading to a build-up of an electron-hole plasma that screens the built-in field.[58] That results in a blue shift compensating for the red shift induced by QCSE, and the large injection current induced blue shift is hence explained. We also note another interesting phenomenon. The GaN-graphene LED demonstrates redshifts of about 4.9 nm and 4 nm at 20 mA and 100 mA, respectively, as compared with the pristine and ITO coated GaN LEDs (see Fig. 5e). Also, for the graphene coated sample, the full width at half maximum (FWHM) of the emission peak is wider than those of graphene-free LEDs. We attribute those effects to the growth process of graphene. Even though the graphene growth temperature has been reduced to 600 °C, there may still be a small degree of indium segregation occurring in the GaN. In other words, In diffusion makes the interfaces between the wells and barriers in the MQW not as abrupt as before. Some amount of In leaves the wells and enters the barriers, resulting in the overall reduction of the InGaN bandgap, which in turn translates into a red shift of the GaN-graphene LED. As the interlayer diffusion can not be absolutely uniform, the several quantum wells are not as identical as before, naturally leading to an enlarged FWHM.

It is well known that higher operating temperatures of LEDs simply means higher junction temperatures, which can cause the light output power of the LEDs to decay, thereby reducing the lifetime.[59,60] Graphene is believed to have the highest thermal conductivity of any known, and presently synthesizable materials.[61] It has shown demonstrable potential as an effective heat spreader in various thermal applications.[62–65] In fact, unlike ITO, graphene has a high potential as the heat spreader in LEDs.[66–68] It may positively augment the thermal management of GaN LEDs, which is explored here. Fig. 6a–f shows thermal maps (SC7300M F/2 (MCT) thermal imaging camera FLIR Systems) on the samples of Fig. 4 operating at 20 mA and 100 mA in constant current mode. Fig. 6g and h is a summary of the temperature distribution along the line from the p electrode to the n electrode of the LEDs as shown in Fig. 6a–f, with the horizontal axis being the coordinates of the line. At 20 mA, compared to room temperature, the temperature increase of the GaN-graphene LED is 0.55–1.2 °C (in average 0.86 °C). The pristine GaN LED and the ITO coated LED increase by 0.86–1.76 °C and 0.63–1.61 °C (in average 1.24 °C and 1.05 °C), respectively. Clearly, by incorporating graphene, it has reduced the temperature increase by a significant 30.6% as compared with the pristine GaN LED. When the current is raised to 100 mA, the GaN-graphene LED temperature increases by 9.85–12.29 °C (in average 10.97 °C), while the pristine and ITO coated GaN LEDs increase by 12.29–16.28 °C and 10.70–14.92 °C, respectively (in average 13.88 °C and 12.54 °C). Evidently, there is a strong thermal spreading effect from the graphene. We conclude that the as-grown graphene has played a significantly positive role in the cooling of GaN LEDs, both at smaller and higher currents, but with a more pronounced effect towards higher injection current in particular. The results indicate that our directly grown graphene technology may be especially useful for high power density GaN based LEDs (*e.g.* extremely high pixel density micro-LED displays).

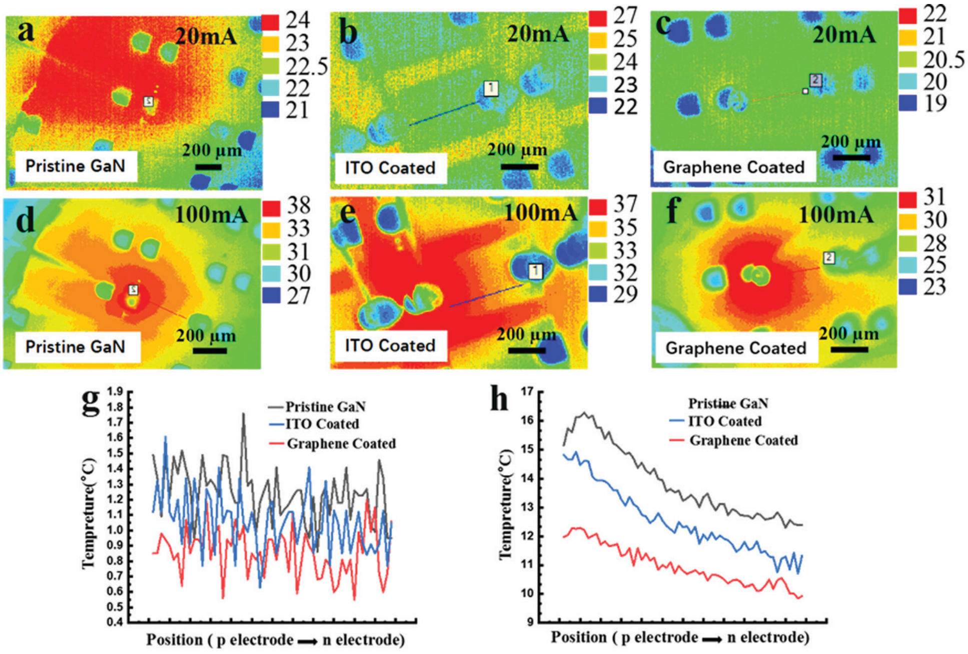

Fig. 6 (a–f) Thermal maps of the three types of GaN LEDs operating at 20 mA and 100 mA. (g and h) The temperature increase of the GaN LEDs at 20 mA and 100 mA (compared to room temperature).

Published on 30 March 2022. Downloaded by University of Bath on 4/11/2022 1:39:27 PM.

4. Conclusion

In summary, we have demonstrated, for the first time, a practical and deployable method for the production of transfer-free patterned graphene directly grown by PECVD on GaN LED epiwafers. The developed process has been seen to be the GaN process compatible through the use of low graphene synthesis temperatures of only 600 °C and the use of dual-functionality Co which catalyzes graphene growth and also functions as an effective GaN dry etching hard mask, which successfully bypasses the complicated problem of the graphene transfer process in the traditional fabrication process, dramatically improving the reproducibility. Also, because graphene grows only on pre-patterned Co, there is no need for additional graphene patterning, eliminating the possibility for graphene to encounter any photolithography, which avoids it from being contaminated and doped by the photoresist. The graphene growth temperature is reduced by virtue of the plasma enhancement technique. Our vertical cold wall CVD system offers the possibility of growing graphene in merely 2 min, and the entire graphene growth process (even including heating and cooling) takes less than 25 min. Based on the study on the effects of different plasma powers and growth time, we have confirmed that 2 min and 40 W AC (15 kHz) plasma are the best growth conditions for the deposition of graphene. Consequently, high-quality graphene is obtained *in situ* on the GaN LED epiwafers with an average optical transmission of 91.74% from 400 nm to 1000 nm wavelength. Comprehensive electrical, optical and thermal analysis of the GaN-graphene LEDs produced by this method have been conducted. The integrated GaN-graphene LEDs demonstrate improved current spreading, current injection and heat spreading functionalities. Unlike other works on graphene application in GaN optoelectronic devices, this facile method is fundamentally scalable, reproducible, controllable, and compatible with current semiconductor planar processing, which is suitable for massive device production towards real applications whilst contributing to the deployment of graphene as a sustainable ITO alternative.

Author contributions

F. X. fabricated the device and conducted the measurements and data analysis. J. S. contributed to data analysis and helped write the paper. M. T. C. and W. G. helped revise the paper. C. Y. and Y. D. and L. W. and Z. D. participated in the experimental design. S. F. and X. L. provided some experimental equipments. T. G. and Q. Y participated in the discussion. All the authors discussed the results and commented on the manuscript.

Data availability

Data are available on request from the authors.

Conflicts of interest

The authors declare no competing interests.

Acknowledgements

This work was supported by the Fujian provincial projects (2021HZ0114, 2021J01583, 2021L3004), the Fujian Science & Technology Innovation Laboratory for Optoelectronic Information of China (2021ZZ122, 2020ZZ110), the National Key R&D Program of China (2018YFA0209004), and the Beijing Municipal Commission of Education (KM201810005029).

Notes and references

1 G. Li, W. Wang, W. Yang, Y. Lin, H. Wang, Z. Lin and S. Zhou, GaN-based light-emitting diodes on various substrates: a critical review, *Rep. Prog. Phys.*, 2016, **79**, 056501.

2 D. Zhu, D. J. Wallis and C. J. Humphreys, Prospects of III-nitride optoelectronics grown on Si, *Rep. Prog. Phys.*, 2013, **76**, 106501.

3 S. F. Chichibu, A. Uedono, T. Onuma, B. A. Haskell, A. Chakraborty, T. Koyama, P. T. Fini, S. Keller, S. P. DenBaars and J. S. Speck, *et al.*, Origin of defect-insensitive emission probability in In-containing (Al, In, GaN) alloy semiconductors, *Nat. Mater.*, 2006, **5**, 810–816.

4 S. Nakamura, The roles of structural imperfections in InGaN-based blue light-emitting diodes and laser diodes, *Science.*, 1998, **281**, 956–961.

5 F. Lang, M. A. Gluba, S. Albrecht, J. Rappich, L. Korte, B. Rech and N. H. Nickel, Perovskite solar cells with large-area CVD-graphene for tandem solar cells, *J. Phys. Chem. Lett*, 2015, **6**, 2745–2750.

6 U. K. Mishra, P. Parikh and Y. Wu, AlGaN/GaN HEMTs-an overview of device operation and applications, *Proc. IEEE.*, 2002, **90**, 1022–1031.

7 K. Wu, T. Wei, D. Lan, H. Zheng, J. Wang, Y. Luo and J. Li, Large-scale SiO_2 photonic crystal for high efficiency GaN LEDs by nanospherical-lens lithography, *Chin. Phys. B*, 2014, **23**, 028504.

8 H. Amano, M. Kito, K. Hiramatsu and I. Akasaki, P-type conduction in Mg-doped GaN treated with low-energy electron-beam irradiation (LEEBI), *Jpn. J. Appl. Phys.*, 1989, **28**, 2112–2114.

9 S. Nakamura, T. Mukai, M. Senoh and N. Lwasa, Thermal annealing effects on p-type Mg-doped GaN films, *Jpn. J. Appl. Phys.*, 1992, **31**, 139–142.

10 J. Neugebauer and C. G. Vandewalle, Role of hydrogen in doping of GaN, *Appl. Phys. Lett.*, 1996, **68**, 1829–1831.

11 K. Novoselov, A. Geim, S. Morozov, D. Jiang, Y. Zhang, S. Dubonos, I. Grigorieva and A. Firsov, Electric field effect in atomically thin carbon films, *Science.*, 2004, **306**, 666–669.

12 R. R. Nair, P. Blake, A. N. Grigorenko, K. S. Novoselov, T. J. Booth, T. Stauber, N. M. R. Peres and A. K. Geim, Fine structure constant defines visual transparency of graphene, *Science.*, 2008, **320**, 1308.

13 K. F. Mak, M. Y. Sfeir, Y. Wu, C. H. Lui, J. A. Misewich and T. F. Heinz, Measurement of the optical conductivity of graphene, *Phys. Rev. Lett.*, 2008, **101**, 196–199.

Published on 30 March 2022. Downloaded by University of Bath on 4/11/2022 1:39:27 PM.

14 L. A. Falkovsky, Optical properties of graphene, *J. Phys. Conf. Ser.*, 2008, **129**, 012004.

15 C. Lee, X. Wei, J. W. Kysar and J. Hone, Measurement of the elastic properties and intrinsic strength of monolayer graphene, *Science.*, 2008, **321**, 385–388.

16 K. I. Bolotin, K. J. Sikes, Z. Jiang, M. Klima, G. Fudenberg, J. Home, P. Kim and H. L. Stormer, Ultrahigh electron mobility in suspended graphene, *Solid State Commun.*, 2008, **146**, 351–355.

17 N. Han, T. V. Cuong, M. Han, B. D. Ryu, S. Chandramohan, J. B. Park, J. H. Kang, Y. J. Park, K. B. Ko and H. Y. Kim, *et al.*, Improved heat dissipation in gallium nitride light-emitting diodes with embedded graphene oxide pattern, *Nat. Commun.*, 2013, **4**, 1452.

18 Z. Zhan, J. Sun, L. Liu, E. Wang, E. Wang, Y. Cao, N. Lindvall, G. Skoblin and A. Yurgens, Pore-free bubbling delamination of chemical vapor deposited graphene from copper foils, *J. Mater. Chem. C*, 2015, **3**, 8634–8641.

19 J. Sun, N. Lindvall, M. T. Cole, K. T. T. Angel, T. Wang, K. B. K. Teo, D. H. C. Chua, J. Liu and A. Yurgens, Low partial pressure chemical vapor deposition of graphene on copper, *IEEE Trans. Nanotechnol.*, 2012, **11**, 255–260.

20 B. J. Kim, C. Lee, Y. Jung, K. H. Baik, M. A. Mastro, J. K. Hite, C. R. Eddy Jr and J. Kim, Large-area transparent conductive few-layer graphene electrode in GaN-based ultra-violet light-emitting diodes, *Appl. Phys. Lett.*, 2011, **99**, 143101.

21 C. J. L. De la Rosa, J. Sun, N. Lindvall, M. T. Cole, Y. Nam, M. Loffler, E. Olsson, K. B. K. Teo and A. Yurgens, Frame assisted H_2O electrolysis induced H_2 bubbling transfer of large area graphene grown by chemical vapor deposition on Cu, *Appl. Phys. Lett.*, 2013, **102**, 022101.

22 A. Boscá, J. Pedrós, J. Martínez, T. Palacios and F. Calle, Automatic graphene transfer system for improved material quality and efficiency, *Sci. Rep.*, 2016, **6**, 21676.

23 Y. Lee, S. Bae, H. Jang, S. Jang, S. E. Zhu, S. H. Sim, Y. I. Song, B. H. Hong and J. H. Ahn, Wafer-scale synthesis and transfer of graphene films, *Nano. Lett.*, 2010, **10**, 490–493.

24 J. Kang, D. Shin, S. Bae and B. H. Hong, Graphene transfer: key for applications, *Nanoscale*, 2012, **4**, 5527–5537.

25 X. Wang, L. Tao, Y. Hao, Z. Liu and R. S. Ruoff, Direct delamination of graphene for high-performance plastic electronics, *Small.*, 2014, **10**, 694–698.

26 L. Liu, X. Liu, Z. Zhan, W. Guo, C. Xu, J. Deng, D. Chakarov, P. Hyldgaard, E. Schroder, A. Yurgens and J. Sun, A mechanism for highly efficient electrochemical bubbling delamination of CVD-grown graphene from metal substrates, *Adv. Mater. Interf.*, 2016, **3**, 1500492.

27 L. Wang, W. Liu, Y. Zhang, Z. H. Zhang, S. T. Tan, X. Yi, G. Wang, X. Sun, H. Zhu and H. V. Demir, Graphene-based transparent conductive electrodes for GaN-based light emitting diodes: challenges and countermeasures, *Nano Energy*, 2015, **12**, 419–436.

28 W. Li, G. Cheng, Y. Liang, B. Tian, X. Liang, L. Peng, A. R. H. Walker, D. J. Gundlach and N. V. Nguyen, Broadband optical properties of graphene by spectroscopic ellipsometry, *Carbon.*, 2016, **99**, 348–353.

29 Y. Zhao, G. Wang, H. Yang, T. An, M. Chen, F. Yu, L. Tao, J. Yang, T. Wei and R. Duan, *et al.*, Direct growth of graphene on gallium nitride by using chemical vapor deposition without extra catalyst, *Chin. Phys. B*, 2014, **23**, 096802.

30 M. Furtado and G. Jacob, Study on the influence of annealing effects in GaN VPE, *J. Cryst. Growth.*, 1983, **64**, 257–267.

31 G. Ding, Y. Zhu, S. Wang, Q. Gong, L. Sun, T. Wu, X. Xie and M. Jiang, Chemical vapor deposition of graphene on liquid metal catalysts, *Carbon.*, 2013, **53**, 321–326.

32 W. Zhang, P. Wu, Z. Li and J. Yang, First-principles thermodynamics of graphene growth on Cu surfaces, *J. Phys. Chem. C*, 2011, **115**, 17782–17787.

33 Y. Zheng, L. Jian, Z. Peng, Z. Sun and J. M. Tour, Toward the synthesis of wafer scale single-crystal graphene on copper foils, *ACS Nano*, 2012, **6**, 9110–9117.

34 Y. Yamazaki, M. Wada, M. Kitamura, M. Katagiri, N. Sakuma, T. Saito, A. Isobayashi, M. Suzuki, A. Sakata and A. Kajita, *et al.*, Low-temperature graphene growth originating at crystalline facets of catalytic metal, *Appl. Phys. Express.*, 2012, **5**, 5101.

35 J. Kim, M. Ishihara, Y. Koga, K. Tsugawa, M. Hasegawa and S. Lijima, Low-temperature synthesis of large-area graphene-based transparent conductive films using surface wave plasma chemical vapor deposition, *Appl. Phys. Lett.*, 2011, **98**, 490.

36 B. Hu, H. Ago, Y. Ito, K. Kawahara, M. Tsuji, E. Magome, K. Sumitani, N. Mizuta, K. I. Ikeda and S. Mizuno, Epitaxial growth of large-area single-layer graphene over Cu(111)/sapphire by atmospheric pressure CVD, *Carbon*, 2012, **50**, 57–65.

37 R. S. Weatherup, B. Dlubak and S. Hofmann, Kinetic control of catalytic CVD for high-quality graphene at low temperatures, *ACS Nano*, 2012, **6**, 9996–10003.

38 L. Gao, W. Ren, H. Xu, L. Jin, Z. Wang, T. Ma, Z. Zhang, Q. Fu and L. Peng, *et al.*, Repeated growth and bubbling transfer of graphene with millimetre-size single-crystal grains using platinum, *Nat. Commun.*, 2012, **3**, 699.

39 J. Wintterlin and M. L. Bocquet, Graphene on metal surfaces, *Surf. Sci.*, 2009, **603**, 1841–1852.

40 J. Sun, Y. Nam, N. Lindvall, M. T. Cole, K. B. K. Teo, Y. W. Park and A. Yurgens, Growth mechanism of graphene on platinum: surface catalysis and carbon segregation, *Appl. Phys. Lett.*, 2014, **104**, 152107.

41 R. S. Weatherup, B. C. Bayer, R. Blume, C. Ducati, C. Baehtz, R. Schlögl and S. Hofmann, In situ characterization of alloy catalysts for low-temperature graphene growth, *Nano Lett.*, 2011, **11**, 4154–4160.

42 R. S. Weatherup, B. C. Bayer, R. Blume, C. Baehtz, P. R. Kidambi, M. Fouquet, C. T. Wirth, R. Schlögl and S. Hofmann, On the mechanisms of Ni-catalysed graphene chemical vapour deposition, *ChemPhysChem*, 2012, **13**, 2544–2549.

43 H.-A. Mehedi, B. Baudrillart, D. Alloyeau, O. Mouhoub, C. Ricolleau, V. D. Pham, C. Chacon, A. Gicquel, J. Lagoute and S. Farhat, Synthesis of graphene by cobalt-catalyzed decomposition of methane in plasma-enhanced

This journal is © The Royal Society of Chemistry 2022

Published on 30 March 2022. Downloaded by University of Bath on 4/11/2022 1:39:27 PM.

CVD: optimization of experimental parameters with Taguchi method, *J. Appl. Phys.*, 2016, **120**, 065304.

44 J. Sawahata, H. Bang, M. Takiguchi, J. Seo, H. Yanagihara, E. Kita and K. Akimoto, Structural and magnetic properties of Co doped GaN, *Phys. Status Solidi C*, 2005, **2**, 2458–2462.

45 R. Wenzel, G. G. Fischer and R. Schmid Fetzer, Ohmic contacts on p-GaN (Part I): investigation of different contact metals and their thermal treatment, *Mater. Sci. Semicond. Process.*, 2001, **4**, 357–365.

46 O. Sul, K. Kim, E. Choi, J. Kil, W. Park and S. B. Lee, Reduction of hole doping of chemical vapor deposition grown graphene by photoresist selection and thermal treatment, *Nanotechnology*, 2016, **27**, 505205.

47 Y. Dong, S. Guo, H. Mao, C. Xu, Y. Xie, J. Deng, L. Wang, Z. Du, F. Xiong and J. Sun, In situ growth of CVD graphene directly on dielectric surface toward application, *ACS Appl. Electron. Mater.*, 2020, **2**, 238–246.

48 A. C. Ferrari, J. C. Meyer, V. Scardaci, C. Casiraghi, M. Lazzeri, F. Mauri, S. Piscanec, D. Jiang, K. S. Novoselov and S. Roth, *et al.*, Raman spectrum of graphene and graphene layers, *Phys. Rev. Lett.*, 2006, **97**, 187401.

49 Z. Ni, Y. Wang, T. Yu and Z. Shen, Raman spectroscopy and imaging of graphene, *Nano Res.*, 2008, **1**, 273–291.

50 I. Calizo, I. Bejenari, M. Rahman, G. Liu and A. A. Balandin, Ultraviolet Raman microscopy of single and multilayer graphene, *J. Appl. Phys.*, 2009, **106**, 043509.

51 M. M. Lucchese, F. Stavale, E. H. M. Ferreira, C. Vilani, M. V. O. Moutinho and R. B. Capaz, Quantifying ion-induced defects and Raman relaxation length in graphene, *Carbon.*, 2010, **48**, 1592–1597.

52 H. K. Kim, C. Mattevi, M. R. Calvo, J. C. Oberg, L. Artiglia, S. Agnoli, C. F. Hirjibehedin, M. Chhowalla and E. Saiz, Activation energy paths for graphene nucleation and growth on Cu, *ACS Nano*, 2012, **6**, 3614.

53 C. J. Rosa, J. Sun, N. Lindvall, M. T. Cole, Y. Nam, M. Loeftier, E. Olsson, K. B. K. Teo and A. Yurgens, Frame assisted H_2O electrolysis induced H_2 bubbling transfer of large area graphene grown by chemical vapor deposition on Cu, *Appl. Phys. Lett.*, 2013, **102**, 22101.

54 E. Loginova, N. C. Bartelt, P. J. Feibelman and K. F. Mccarty, Factors influencing graphene growth on metal surfaces, *New J. Phys.*, 2009, **11**, 063046.

55 L. Gao, J. R. Guest and N. P. Guisinger, Epitaxial graphene on Cu(111), *Nano Lett.*, 2010, **10**, 3512–3516.

56 J. Sun, M. T. Cole, S. A. Ahmad, O. Backe, T. Ive, M. Loffler, N. Lindvall, E. Olsson, K. B. K. Teo and J. Liu, *et al.*, Direct chemical vapor deposition of large-area carbon thin films on gallium nitride for transparent electrodes: a first attempt, *IEEE Trans. Semicond. Manuf.*, 2012, **25**, 494–501.

57 M. B. Dutt and V. Mittal, Investigation of electrical transport properties of as-implanted silicon for making micromachined uncooled bolometric arrays, *J. Appl. Phys.*, 2005, **97**, 083704.

58 G. Traetta, A. D. Carlo, A. Reale, P. Lugli, M. Lomascolo, A. Passaseo, R. Cingolani, A. Bonfiglio, M. Berti and E. Napolitani, *et al.*, Charge storage and screening of the internal field in GaN/AlGaN quantum wells, *J. Cryst. Growth.*, 2001, **230**, 492–496.

59 J. J. Fu, L. Zhao, H. Cao, X. Sun, B. Sun, J. Wang and J. Li, Degradation and corresponding failure mechanism for GaN-based LEDs, *AIP Adv.*, 2016, **6**, 055219.

60 S. C. Yang, P. Lin, C. P. Wang, S. B. Huang, C. L. Chen, P. F. Chiang, A. T. Lee and M. T. Chu, Failure and degradation mechanisms of high-power white light emitting diodes, *Microelectron. Reliab.*, 2010, **50**, 959–964.

61 A. A. Balandin, S. Ghosh, W. Bao, I. Calizo, D. Teweldebrhan, F. Miao and C. N. Lau, Superior thermal conductivity of single-layer graphene, *Nano Lett.*, 2008, **8**, 902.

62 G. Xin, T. Yao, H. Sun, S. M. Scott, D. Shao, G. Wang and J. Lian, Highly thermally conductive and mechanically strong graphene fibers, *Science.*, 2015, **349**, 1083–1087.

63 C. T. Hsieh, C. E. Lee, Y. F. Chen, J. K. Chang and H. S. Teng, Thermal conductivity from hierarchical heat sinks using carbon nanotubes and graphene nanosheets, *Nanoscale*, 2015, **7**, 18663–18670.

64 G. Xin, H. Sun, T. Hu, H. R. Fard, X. Sun, N. Koratkar, T. Borca-Tasciuc and J. Lian, Large-area freestanding graphene paper for superior thermal management, *Adv. Mater.*, 2014, **26**, 4521–4526.

65 Y. Kuang, L. Lindsay and B. Huang, Unusual enhancement in intrinsic thermal conductivity of multilayer graphene by tensile strains, *Nano Lett.*, 2015, **15**, 6121–6127.

66 Y. H. Lee and J. H. Lee, Scalable growth of free-standing graphene wafers with copper (Cu) catalyst on SiO_2/Si substrate: thermal conductivity of the wafers, *Appl. Phys. Lett.*, 2010, **96**, 083101.

67 Z. Wang, L. I. Guang-Ji and H. Feng, Study on the preparation and properties of transparent and heat-insulating EVA/ITO materials, *Synth. Mater. Aging Appl.*, 2009, **38**, 12–16.

68 N. Han, T. V. Cuong, M. Han, B. D. Ryu, S. Chandramohan, J. B. Park, J. H. Kang, Y. J. Park, K. B. Ko and H. Y. Kim, *et al.*, Improved heat dissipation in gallium nitride light-emitting diodes with embedded graphene oxide pattern, *Nat. Commun.*, 2013, **4**, 1452.

This journal is © The Royal Society of Chemistry 2022